Apoptosis (2019) 24:905–920
https://doi.org/10.1007/s10495-019-01568-2

Oroxylin A induces apoptosis of activated hepatic stellate cells through endoplasmic reticulum stress

Mianli Bian[1,3,4] · Jianlin He[1,2] · Huanhuan Jin[1,5] · Naqi Lian[1,3,4] · Jiangjuan Shao[1,3,4] · Qinglong Guo[6] · Shijun Wang[7] · Feng Zhang[1,3,4] · Shizhong Zheng[1,3,4]

Published online: 20 September 2019

Abstract

Hepatic stellate cell (HSC) activation plays an indispensable role in hepatic fibrosis. Inducing apoptosis of activated HSCs can attenuate or reverse fibrogenesis. In this study, we initially found that oroxylin A (OA) protected CCl_4-induced liver injury accompanied by endoplasmic reticulum stress (ERS) activation of HSCs in mice. In vitro, OA treatment markedly reduced fibrogenesis by modulating extracellular matrix synthesis and degradation. OA inhibited cell proliferation and induced cell cycle arrest of HSCs at S phase. Further, OA was observed to induce HSC apoptosis, as indicated by caspase activation. Using the eIF2α dephosphorylation inhibitor salubrinal, we found that ERS pathway activation was required for OA to induce HSC apoptosis. ERS-related proteins were significantly upregulated by OA treatment, and salubrinal abrogated the effects of OA on HSCs. Thus, we inferred that OA attenuated HSC activation by promoting ERS. In vivo, inhibition of ERS by salubrinal partly abrogated the hepatoprotective effect of OA in CCl_4-treated mice. In conclusion, our findings suggest a role for ERS in the mechanism underlying amelioration of hepatic fibrosis by OA.

Keywords Oroxylin A · Hepatic stellate cell · Apoptosis · Endoplasmic reticulum stress

Introduction

Hepatic fibrosis, a reversible process that occurs during healing of insults to the liver, is characterized by hepatic stellate cell (HSC) activation, which is accompanied by massive accumulation of extracellular matrix (ECM), especially the production of collagen [1]. Hepatic fibrosis is induced by multiple factors, including alcohol consumption, chronic viral hepatitis, fatty liver, cholestasis, and autoimmune hepatitis, which cause excessive ECM deposition and hypertrophic scarring [2]. Persistent fibrosis causes cirrhosis and even hepatocellular carcinoma. Currently, liver transplantation is considered the most feasible and effective method to treat end-stage cirrhosis.

Under normal physiological conditions, HSCs are in a resting state and their major function is storage of vitamin A and retinoic acid [3]. Platelet-derived growth factor (PDGF)

Electronic supplementary material The online version of this article (https://doi.org/10.1007/s10495-019-01568-2) contains supplementary material, which is available to authorized users.

Mianli Bian and Jianlin He contributed equally to this work.

✉ Feng Zhang
nucmzf@163.com

✉ Shizhong Zheng
szhengnucm@163.com; nytws@njucm.edu.cn

[1] Department of Pharmacology, School of Pharmacy, Nanjing University of Chinese Medicine, 138 Xianlin Avenue, Nanjing 210023, Jiangsu, China

[2] Third Institute of Oceanography, Ministry of Natural Resources, 361005 Xiamen, China

[3] Jiangsu Key Laboratory for Pharmacology and Safety Evaluation of Chinese Materia Medica, Nanjing University of Chinese Medicine, Nanjing, Jiangsu, China

[4] Jiangsu Key Laboratory for Functional Substance of Chinese Medicine, Nanjing University of Chinese Medicine, Nanjing, Jiangsu, China

[5] Department of Pharmacology, School of Pharmacy, Wannan Medical College, Wuhu 241000, China

[6] Jiangsu Key Laboratory of Carcinogenesis and Intervention, China Pharmaceutical University, Nanjing, China

[7] Shandong Co-innovation Center of TCM Formula, College of Traditional Chinese Medicine, Shandong University of Traditional Chinese Medicine, 138 Xianlin Avenue, Nanjing 210023, Jiangsu, China

and epidermal growth factor (EGF) induce activation and proliferation of HSCs, which adopt a fibroblast-like phenotype [3, 4]. HSC activation is highly promoted during the process of hepatic fibrosis, and induction of activated HSC apoptosis has been shown to be an effective strategy to promote recovery from fibrosis [5]. Apoptosis mostly occurs via a mitochondrial system and death-receptor pathways, but also occurs in response to cellular activities such as endoplasmic reticulum stress (ERS) [6]. The endoplasmic reticulum (ER) is an important organelle necessary for cell survival and normal cellular functions. ERS plays a vital role in the mechanism of cell clearance, which is also mediated by death receptor and mitochondrial pathways [7]. Folded proteins are transported to the Golgi apparatus, where accumulation of many unfolded proteins further aggravates ERS, which are degraded by the proteasome [8]. However, little is known about the role of ERS in apoptosis during hepatic fibrosis. Therefore, it is vital to investigate mechanisms of apoptotic signaling pathways in activated HSCs.

Oroxylin A (OA) widely exists in plants and is derived from the natural flavonoid molecule wogonin [9]. In recent years, OA has attracted great attention for its emerging role in treating liver cancer [10]. Inducing apoptosis of activated HSCs is an effective strategy to treat hepatic fibrosis. Therefore, the aim of the current research was to investigate the effects of OA on apoptosis during HSC activation, and to further examine the underlying mechanisms.

Materials and methods

Reagents and antibodies

OA of a purity higher than 99% was isolated from the medicinal plant *Scutellaria baicalensis* and dissolved in dimethyl sulfoxide (DMSO) [9]. The control group was treated with 0.1% DMSO. Salubrinal was purchased from Sigma (St Louis, MO, USA), dissolved in DMSO, and stored at − 20 °C. For western blot analyses, primary antibodies against caspase-3, -7, -8, and -9; poly (ADP-ribose) polymerase (PARP); cytochrome c; Bax; and Bcl-2; as well as all secondary antibodies were obtained from Cell Signaling Technology (Danvers, MA, USA). Antibodies against calnexin, C/EBP homologous protein (CHOP), protein kinase RNA-like endoplasmic reticulum kinase (PERK), inositol-requiring enzyme-1 (IRE1), and activating transcription factor 6 (ATF6) were purchased from Wan Lei Biology Antibody (Shenyang, China). The anti-β-actin antibody was purchased from Sigma. Antibodies against fibronectin, α-smooth muscle actin (α-SMA), and α1(I) procollagen were purchased from Epitomics (San Francisco, CA, USA). Primers used for quantitative real-time polymerase chain reactions (qRT-PCR) were purchased from GenScript Co. Ltd. (Nanjing, Jiangsu, China). Phosphate-buffered saline (PBS), Dulbecco's Modified Essential Medium (DMEM), fetal bovine serum (FBS) and trypsin-EDTA were purchased from Gibco BRL (Grand Island, NY, USA).

Animals and experimental procedures

All experiment protocols involving mice (Yangzhou University, China) were approved by institutional and local ethics committees. In accordance with National Institutes of Health (Bethesda, MD, USA) guidelines, all mice received humane care. 5-week-old male ICR mice (18–22 g) were randomly divided into eight groups (n = 8). All animals were housed under standardized conditions at room temperature, with suitable humidity and light/dark cycle with dawn/dusk effect. Water and standard pathogen-free chow diet were provided ad libitum [11]. A mixture of carbon tetrachloride (CCl_4; 0.5 mL/100 g body weight) and olive oil [1:9 (v/v)] was used to induce liver fibrosis in mice by intraperitoneal injection. Group 1 was the vehicle control, in which mice did not receive CCl_4 or OA treatment. Group 2 was the CCl_4 model group. Groups 3, 4, and 5 were drug treatment groups, in which mice received CCl_4 and OA at 20, 30, or 40 mg/kg, respectively. Group 6 was the positive control group, in which mice received CCl_4 and colchicine treatment (0.1 mg/kg). Group 7 received an intraperitoneal injection of salubrinal at 1 mg/kg. Group 8 received salubrinal and OA at the same time. Groups 2–8 were injected with CCl_4 (5 mL/kg) twice a week for 8 weeks to induce hepatic fibrosis. Groups 3–8 were intraperitoneally injected with OA or salubrinal daily for the last 4 weeks. OA, salubrinal, and colchicine were dissolved in physiological saline. After 8 weeks of administration, blood and livers were collected. Livers were fixed in 4% buffered paraformaldehyde for histological analysis and western blot analysis.

Cell culture conditions

The HSC-T6 rat hepatic stellate cell line (Cell Bank of Chinese Academy of Sciences, Shanghai, Chinese) was cultured in DMEM containing 10% FBS and 1% antibiotics, in a 95% air 5% CO_2 humidified atmosphere at 37 °C. A Leica Qwin System (Wetzlar, Germany) was used to observe HSC morphology [6].

Quantitative real-time polymerase chain reaction

TRIzol reagent was used to extract HSC RNA according to the manufacturer's instructions. Real-time PCR was carried out using a 7500 RT-PCR System as previously described [12]. mRNA levels of target genes were calculated and reported from triplicate experiments. The following primers (GenScript, Nanjing, China) were used:

GAPDH: (forward) 5′-TGGTATCGTGGAAGGACTCAT GAC-3′, (reverse) 5′-ATGCCAGTGAGCTTCCCGTTC AGC-3′; CHOP: (forward) 5′-AGCAGAGGTCACAAG CACCT-3′, (reverse) 5′-CTCCTTCATGCGCTGTTT CC-3′; calnexin: (forward) 5′-GATGCTGTCAAGCCA GATGA-3′, (reverse) 5′-TTAGGGTTGGCAATCTGA GG-3′; Bcl-2: (forward) 5′-TTCGGGATGGAGTAAACT GG-3′; (reverse) 5′-AAGGCTCTAGGTGGTCATTCAG-3′; Bax: (forward) 5′-TGGAGATGAACTGGACAGCA-3′; (reverse) 5′-CAAAGTAGAAGAGGGCAACCAC-3′; type I collagen: (forward) 5′-ACGTCCTGGTGAAGTTGG TC-3′; (reverse) 5′-TCCAGCAATACCCTGAGGTC-3′; α-SMA: (forward) 5′-TCTCACCGACTACC-3′, (reverse) 5′-TCCAGAGCGACATAGCACAG-3′.

Immunoblotting analysis

Cell lysates were prepared using RIPA buffer containing protease and phosphatase inhibitors. A bicinchoninic acid assay kit was used to determine protein levels (Pierce, Thermo Fisher Scientific, Waltham, MA, USA). Proteins were electrophoresed and transferred to a polyvinylidene difluoride membrane (Millipore, Burlington, MA, USA), which was blocked with 5% skim milk for 2 h. Subsequently, membranes were incubated with primary antibodies overnight followed by conjugated secondary antibodies for 2 h the following day. A chemiluminescence reagent (Millipore) was used to detect antibody binding. β-actin was used as a reference protein to determine levels of target proteins densitometrically with Quantity One software (Bio-Rad, Hercules, CA, USA).

Immunofluorescence analysis

Liver tissues or treated HSCs underwent immunofluorescence analysis as previously reported [13], with 4′,6-diamidino-2-phenylindole (DAPI) to stain nuclei. Briefly, HSCs were seeded in 24-well plates and cultured for 24 h, followed by treatment with OA or salubrinal for another 24 h. Subsequently, HSCs were incubated with primary antibody at 4 °C overnight, followed by anti-rabbit or anti-mouse IgG for 2 h at room temperature, and then washed with PBS three times. Immunofluorescence was detected with a fluorescence microscope (Nikon, Tokyo, Japan). For liver tissues, sections (5 μm) were blocked with 1% bovine serum albumin and incubated with primary antibodies overnight at 4 °C overnight, followed by incubation with secondary antibodies for another 2 h at room temperature. Sections were washed three times with PBS between reagents. Immunofluorescence was detected in a single plane using an MRC 1024 laser confocal microscope (Bio-Rad).

Enzyme-linked immunosorbent assay (ELISA)

ELISA kits were used to determine serum levels of tumor necrosis factor (TNF)-α, interleukin 6 (IL-6), IL-8, hyaluronic acid (HA), laminin (LN), procollagen type III (PCIII), and type IV collagen (Col IV) according to the manufacturer's protocols (Sen Bei Jia Biological Technology, Nanjing, China). Absorbance was observed with a SpectraMax™ microplate spectrophotometer (Molecular Devices, Sunnyvale, CA, USA).

Transmission electron microscopy

Livers were fixed with 1% glutaraldehyde in 0.1 M cacodylate buffer, cut into small pieces, and post-fixed with 4% OsO_4 in the same buffer. Tissue samples were then dehydrated and embedded in epoxy resin (Spurr; Electron Microscopy Sciences, Ft. Washington, PA). An Olympus EM208S transmission electron microscope (Tokyo, Japan) was used to acquire images of tissue sections.

Biochemical analysis

Sera was separated from whole blood and levels of aspartate aminotransferase (AST), alanine aminotransferase (ALT), alkaline phosphatase (ALP), and lactate dehydrogenase (LDH) were determined using commercial assay kits (Nanjing Jiancheng Bioengineering Institute, China) following the manufacturer's protocols. A SpectraMax™ microplate spectrophotometer was used to determine the absorbance values (Molecular Devices).

Cell proliferation assay

HSCs proliferation was tested with a Cell Counting Kit 8 (CCK-8) kit (Dojindo, Japan). Cells were seeded into 96-well plates in a volume of 200 μL per well and cultured overnight at 37 °C. According to the manufacturer's protocol, after treatment with varying concentrations of DMSO or OA for 24 h, 20 μL of CCK-8 solution was added to each well and cells were incubated for 2 h at 37 °C. A scanning multiwell spectrophotometer was then used to determine the absorbance of the each well at 450 nm.

Terminal deoxynucleotidyl transferase (TdT) dUTP nick-end labeling (TUNEL) staining

HSCs were seeded in 24-well plates as described above for 24 h. The next day, cells were treated with DMSO, OA, or salubrinal at the indicated concentrations for another 24 h. Morphology of apoptotic HSCs was evaluated using a

TUNEL staining kit (KeyGen Biotech, Nanjing, China). A fluorescence microscope (Nikon) was used to capture images of HSCs.

Analysis of cell cycle and apoptosis by flow cytometry

HSCs were seeded in six-well plates at a density of 2×10^4 cells/well and cultured for 24 h. Next, HSCs were treated with DMSO or OA at indicated concentrations for another 24 h. Cellular DNA flow cytometry kits (KeyGen Biotech) were used according to the manufacturer's protocol to evaluate the cell cycle stage of cells (specifically G0/G1, S, or G2/M) by flow cytometry (FACS Calibur; BD Biosciences, Franklin Lakes, NJ, USA).

Apoptosis was determined by fluorescein isothiocyanate (FITC)-labeled annexin V/propidium iodide (PI) double staining. An annexin V-FITC apoptosis assay kit (KeyGen Biotech) was used according to the manufacturer's protocol. Percentages of annexin-positive HSCs without PI staining were determined by flow cytometry (FACS Calibur). Data were analyzed using Cell Quest software (BD Biosciences).

Statistical analysis

Data are expressed as mean ± standard deviation and were analyzed using Prism 5.0 (GraphPad Software, La Jolla, CA, USA). Statistical significance of differences was determined by one-way analysis of variance (ANOVA) with post-hoc Dunnett's test. P-values <0.05 were considered statistically significant.

Results

OA protected mouse livers from CCl_4-induced injury and inflammation accompanied by ERS activation

To assess the protective effect of OA, we used a mouse model to explore its therapeutic potential to treat hepatic fibrosis. To this end, we analyzed biochemical markers of liver injury after CCl_4 treatment for 8 weeks. Levels of AST, ALT, ALP, and LDH were effectively increased in Group 2 (the model group) but were reduced by OA in CCl_4-treated mice. Notably, high-dose OA reduced AST and ALT levels more significantly than colchicine (Fig. 1a). During chronic liver disease, inflammation is commonly accompanied by hepatic fibrogenesis. As demonstrated by ELISA results, OA also decreased serum levels of IL-6, IL-8, and TNF-α (Fig. 1b). Thus, we proposed that OA protected the liver against CCl_4-induced injury by suppressing inflammation. In addition, H&E staining showed that treatment with OA significantly improved morphological changes in liver tissue (Fig. 1c). As fibrogenesis is accompanied by accumulation of collagen, liver tissue sections were stained with Masson's reagent and Sirius red to examine collagen deposition. The results indicated that collagen was markedly deposited in the CCl_4-injured liver, but dose-dependently reduced in the livers of mice in OA-treated groups (Fig. 1c). In addition, OA significantly reduced upregulated levels of HA, LN, PC-III, and C-IV in serum by CCl_4 (Fig. 1d). To further confirm these phenomena, we investigated protein expression of three major markers of hepatic fibrosis: α-SMA, α1(I) procollagen, and fibronectin. The results indicated that OA effectively diminished their protein expression (Fig. S1A). Severe inflammatory cell infiltration in livers exposed to CCl_4, characterized by reduced intrahepatic CD45- and F4/80-positive cells, was suppressed by OA (Fig. S1B). These data confirmed that the process of hepatic fibrosis was accompanied by both inflammation and activation of HSCs in vivo.

Interestingly, ultrastructural studies using transmission electron microscopy to observe morphological changes in the ER revealed that OA caused a striking dose-dependent change in the cytosol, such as ER enlargement and characteristic translucent vacuoles [8], indicating that OA activates ERS (Fig. 2a). Considering the results described above, liver sections were used to evaluate expression of α-SMA, a major marker of HSC activation, by immunofluorescence. The results of double staining with α-SMA showed that CHOP and calnexin were increased in HSCs. Specifically, CHOP and calnexin were absent in fibrotic mouse livers but elevated by OA at various doses (Fig. 2b). Together, these data showed that OA could protect mice against liver injury during CCl_4-induced fibrosis in vivo, which was accompanied by ERS activation in HSCs.

OA inhibited HSC proliferation in vitro and induced cell cycle arrest in S phase

We next investigated the effect of OA on HSCs in vitro. Activation and proliferation of HSCs are hallmarks of hepatic fibrosis [14]. Therefore, we initially examined the inhibitory effects of OA on HSC proliferation using a CCK-8 assay. OA dose-dependently inhibited HSC growth and had a significant inhibitory effect at 30 μM (Fig. 3a). Inhibition of HSC viability is necessary for inducing apoptosis of activated HSCs. CCK-8 analysis indicated that OA had a striking anti-proliferative effect on activated HSCs that occurred in a dose- and time- dependent manner (Fig. 3a). As an ideal anti-fibrotic agent should be selective for HSCs without affecting other hepatic cells, we also examined the effect of OA on the human hepatocyte cell line LO_2. Our results showed that OA significantly inhibited the proliferation of LO_2 cells at 70 μM (Fig. 3b), demonstrating that OA had a selective inhibitory effect on HSC growth within a

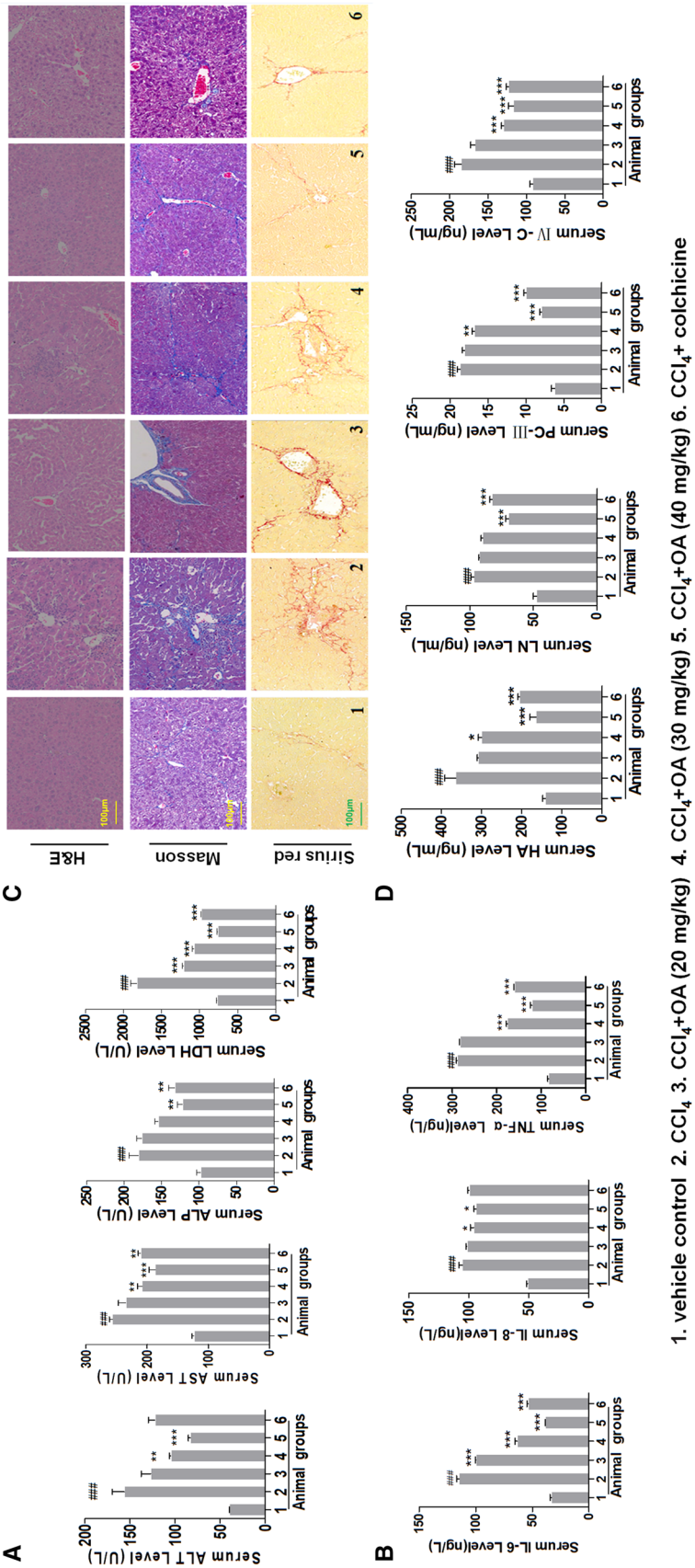

Fig. 1 OA protects mice liver from CCl_4-induced injury and inflammation. Mice were grouped as follows: group one, vehicle control (olive oil); group two, model group (CCl_4); group three, OA (20 mg/kg) and CCl_4-treated group; group four, OA (30 mg/kg) and CCl_4-treated group; group five, OA (40 mg/kg) and CCl_4-treated group; group six, colchicine (0.1 mg/kg) and CCl_4-treated group. n = 8/group. Mice were injected i.p. with CCl_4 for 8 weeks, to induce hepatic fibrosis. **a** Determination of serum ALT, AST, ALP and LDH levels. **b** ELISA measured the levels of IL-6, IL-8 and TNF-α in liver and serum. **c** Liver sections were stained with hematoxylin and eosin, Masson reagents, Sirius red. Representative photographs are shown (original magnification, ×20). **d** Levels of HA, LN, PC-III, and C-IV in serum. For the statistics of each panel in this figure, data are expressed as mean ± SD (n = 8); $^{\#\#}P < 0.001$ compared with group one, $^{*}P < 0.05$, $^{**}P < 0.01$ and $^{***}P < 0.001$ compared with group two

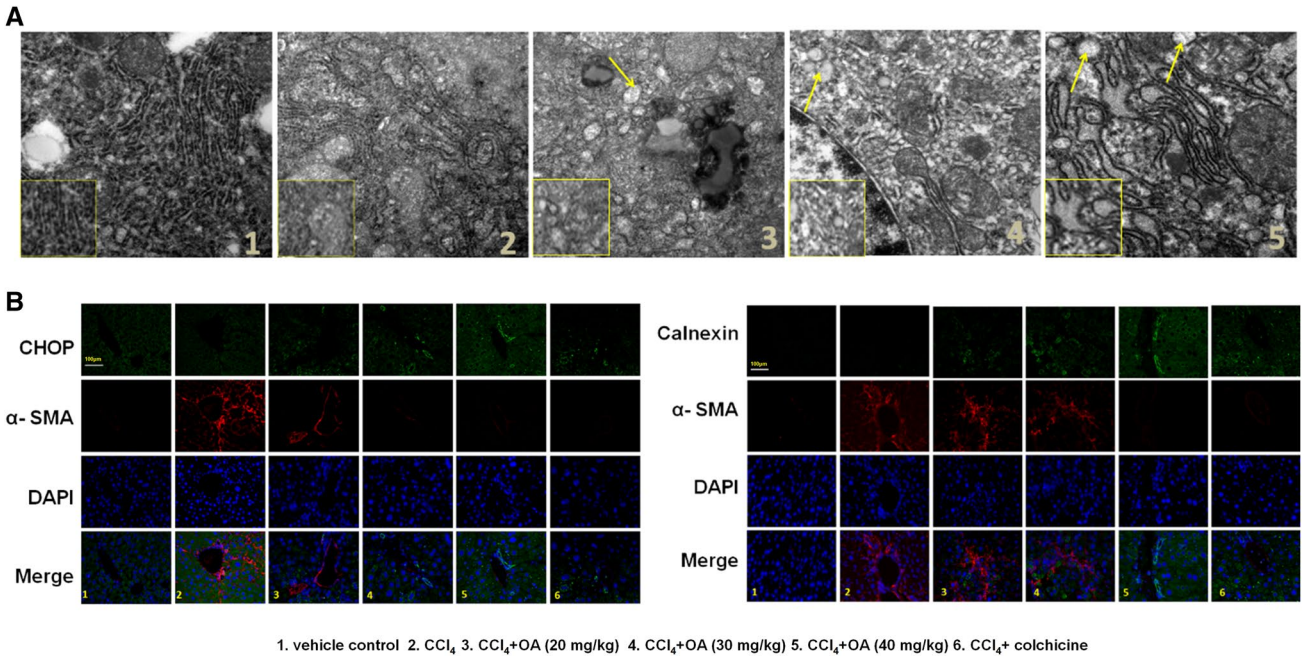

Fig. 2 OA increases ERS in CCl_4-induced injury. Mice were injected i.p. with CCl_4 for 8 weeks, to induce hepatic fibrosis. During the weeks 5–8, mice in treatment groups were treated with OA (20, 30, 40 mg/kg) or colchicine (0.1 mg/kg). **a** Transmission electron microscopy (TEM) showed that OA in a dose-dependent manner caused dramatic morphological changes with appearance of cytoplasmic vacuoles. **b** Liver sections were stained with immunofluorescence using antibodies against CHOP and Calnexin. Antibody against α-SMA was used to specifically stain HSC, and DAPI to stain the nucleus (original magnification, ×40). Scale bar = 100 μm. Scale bar = 100 μm. For the statistics of each panel in this figure, data are expressed as mean ± SD (n = 8); $^{\#\#\#}P < 0.001$ compared with group one, $^{*}P < 0.05$, $^{**}P < 0.01$ and $^{***}P < 0.001$ compared with group two

certain dose range. Furthermore, according to the results of an LDH release assay, OA had cytotoxic effects on LO_2 only at doses higher than 70 μM (Fig. 3b).

Activation of HSCs is accompanied by reactive oxygen species (ROS) generation [15, 16]. Therefore, we evaluated ROS levels in activated HSCs treated with DMSO or OA for 24 h. OA dose-dependently suppressed ROS generation in activated HSCs (Fig. 3c). Moreover, according to flow cytometry analysis, OA dose-dependently induced S-phase accumulation (Fig. 3d, e). Multiple mechanisms potentially underly the inhibition of inappropriate cell proliferation, including the main regulator proteins cyclins, cyclin-dependent-kinases (CDKs), and CDK inhibitors [17]. Cyclin A and cyclin E are central proteins involved in S-phase entry, whereby they induce DNA replication by controlling thymidine kinase and cyclin [18]; notably, cyclin E1 can activate CDK2. Thus, we investigated whether these molecules were modulated by OA treatment. Western blot analysis indicated that OA down-regulated cyclins and CDK expression (Fig. 3f). Furthermore, we observed that OA dose-dependently increased expression of p15, p21, and p27, which regulate cell cycle progression by inhibiting the cyclin-CDK complex (Fig. 3g). Activated HSCs are responsible for increased collagen synthesis and deposition in the liver. HSC activation is accompanied by upregulated expression of PDGF-β, transforming growth factor-β, and EGF receptors, which increase the transduction of profibrogenic signals [19]. OA dose-dependently inhibited the expression of these three receptors and attenuated HSC activation (Fig. 3h). Thus, these results collectively indicated that OA suppressed HSC proliferation and caused cell cycle arrest in S phase by altering levels of the main proteins regulating cell cycle.

OA induced apoptosis of activated HSCs through caspase activation

Induction of apoptosis, which plays an important role in clearing activated HSCs, is characterized by HSC shrinkage, chromatin condensation, and nuclear fragmentation [20]. Therefore, we examined the effects of OA on the progression of apoptosis. As evident by phase contrast microscopy, OA treatment caused dramatic morphological changes in HSCs in a dose-dependent manner, as manifested by cell shrinkage, semi-detachment, and sphere-shaped cells (Fig. 4a). We next explored the pathway underlying OA-induced HSC apoptosis. Flow cytometry demonstrated that OA enhanced apoptosis in activated HSCs in a dose-dependent manner (Fig. 4b). Furthermore, TUNEL staining revealed that OA effectively induced apoptosis in activated HSCs (Fig. 4c).

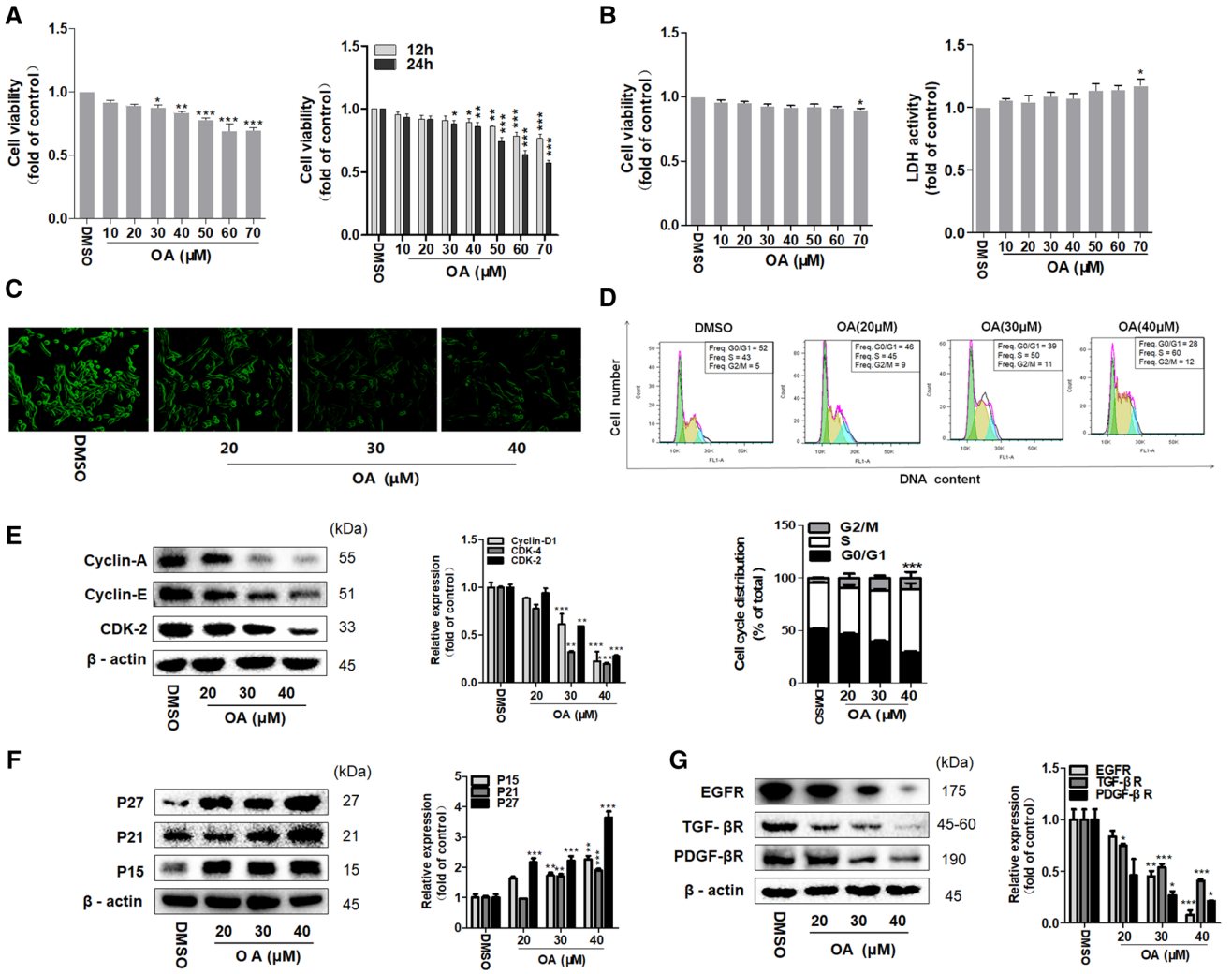

Fig. 3 OA inhibits HSC proliferation and induces cell cycle arrest at the S checkpoint in vitro. Cells were treated with DMSO (0.02%, w/v) and OA for 24 h. **a**, **b** CCK8 assay and LDH release assay. **c** The formation of reactive oxygen species (ROS) was measured using Image-IT™ LIVE Green Reactive Oxygen Species Detection Kit. **d** Cell cycle analysis by flow cytometry. Percentages of cell cycle distributions were determined by flow cytometry. **e**, **f** Western blot analyses of cell cycle regulatory proteins. **g** Protein expression of profibrotic cytokines in HSCs by western blot analyses. β-actin was used as an invariant control for equal loading. Representative blots were from three independent experiments. Data are expressed as mean ± SD (n = 3); *P < 0.05, **P < 0.01 and ***P < 0.001 compared with DMSO

qRT-PCR consistently demonstrated that OA dose-dependently reduced Bcl-2 mRNA levels in HSCs, while increasing Bax mRNA levels; however, RNA expression of these factors was not significantly altered in LO_2 cells (Fig. 4d). Increasing the Bax/Bcl-2 ratio facilitates cytochrome c release into the cytosol and further activates caspase cascades [21]. Therefore, we examined the expression of Bcl-2 family-related proteins localized to the mitochondrial inner membrane. In activated HSCs, OA reduced the level of Bcl-2 and increased the level of Bax, which act as anti-apoptotic and pro-apoptotic proteins, respectively (Fig. 4e). Caspases are produced in cells as catalytically inactive proenzymes, which undergo proteolytic activation during apoptosis [22]. As such, we investigated protein expression levels of both the cleaved active form and inactive pro-form of two caspases [23]. As shown in Fig. 4f, OA dose-dependently upregulated cleaved-caspase-9 and cleaved-caspase-3 without affecting the expression of pro-caspase-9 or pro-caspase-3, suggesting that OA-induced HSC apoptosis was accompanied by caspase activation. Notably, the cleaved form of PARP, a zinc-dependent DNA binding protein that recognizes DNA strand breaks (and marker of apoptosis) [24], was increased by OA, consistent with caspase activation and nuclear morphological changes (Fig. 4f). Caspase-8 activates almost all apoptotic downstream cascades, inducing caspase-7, and leads to the apoptosis of HSCs [25]. Both

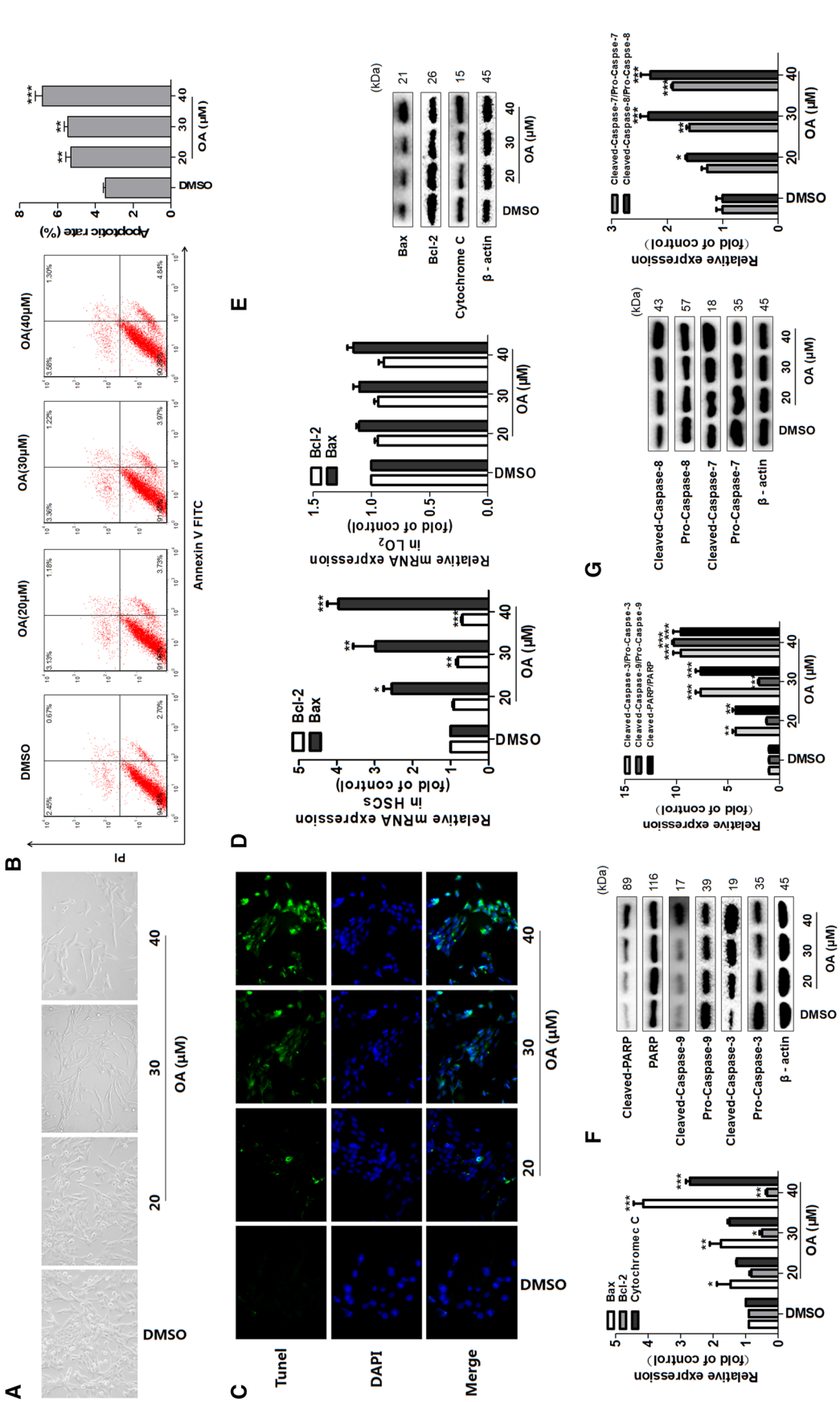

Fig. 4 Effect of OA on the induction of apoptosis in HSCs. **a** Cell morphology assessment. HSCs were treated with DMSO (0.02%, w/v) or OA at indicated concentrations for 24 h (original magnification, ×20). **b** Flow cytometry analyses of HSC apoptosis using FITC-labelled Annexin-V/PI staining. Cells situated in the right two quadrants of each plot were regarded as apoptotic cells. **c** TUNEL staining for evaluating HSC apoptosis. Green fluorescence indicated HSC apoptotic (original magnification, ×40). **d** Real-time PCR analyses of Bcl-2 family genes in HSC and human LO_2 hepatocytes. **e** Western blot analyses of Bcl-2 family proteins in HSC. **f**, **g** Western blot analyses of caspase cascades and PARP-1 in HSC. Data are expressed as mean ± SD (n = 3); *P < 0.05, **P < 0.01 and ***P < 0.001 compared with DMSO

of these caspases were activated by OA in a dose-dependent manner, as determined by western blot analyses (Fig. 4g). These data consistently indicated that OA stimulated apoptosis of activated HSCs.

OA inhibited collagen synthesis and induced collagen degradation in activated HSCs

Next, we evaluated expression of α-SMA, type I collagen, and fibronectin. OA treatment markedly reduced mRNA levels of type I collagen and α-SMA compared with DMSO treatment (Fig. 5a). Western blot results indicated that OA decreased fibronectin, α-SMA, and type I collagen levels (Fig. 5b). Notably, fibrogenesis is greatly influenced by the rate of collagen synthesis in relation to matrix metalloproteinase (MMP) degradation [26]. The actual proteolytic activity of MMPs depends on the ratio of MMPs to their corresponding tissue inhibitor of matrix metalloproteinases (TIMPs) [27]. As such, the balance between MMPs and TIMPs is a key regulator of adaptive and maladaptive responses to ECM production [28]. Thus, we explored whether OA treatment contributed to the regulation of fibrosis by MMPs. As shown in Fig. 5c, western blot analysis suggested that OA treatment increased MMP-9 expression, but inhibited TIMP-2 expression. Thus, the MMPs/TIMPs balance changed during ECM degradation. These alterations were confirmed by immunofluorescence analysis (Fig. 5d). Altogether, these data indicated that OA could improve hepatic fibrosis by both decreasing the expression of ECM proteins and inducing ECM degradation in HSCs.

Activation of the ERS pathway by OA treatment induced apoptosis of activated HSCs

We next investigated the mechanism of OA-induced HSC apoptosis by examining two major mediators of the ERS pathway, calnexin and CHOP, an ER chaperone and major marker of prolonged ERS, respectively [29]. Immunofluorescence showed that OA markedly upregulated expression of CHOP and calnexin (Fig. 6a). Notably, OA at 40 μM significantly upregulated mRNA levels of both calnexin and CHOP in HSCs but did not significantly alter their mRNA expression in LO_2 cells (Fig. 6b). Similar results were observed for protein levels in HSCs by western blot analysis (Fig. 6c). Furthermore, triggered by many physiological and pathophysiological stimuli, the accumulation of unfolded proteins leads to activation of the unfolded protein response, which is mediated by three types of ER transmembrane receptors: PERK, IRE1, and ATF6 [30, 31]. PERK promotes eIF2α phosphorylation as an immediate response, leading to eIF2α activation and decreased mRNA translation, thus resulting in further accumulation of unfolded proteins in the ER [31]. IRE1, an ER transmembrane protein with both kinase and endoribonuclease activity, includes an N-terminal luminal sensor domain, a single transmembrane domain, and C-terminal cytosolic effector region [32]. ATF6 is a regulatory gene that includes sequences with a site referred to as the cAMP response element [29]. The related receptor proteins work together to maintain the balance of ERS and contribute to ER homeostasis during the early stages of ERS. Western blot analyses showed that OA significantly upregulated protein expression of these regulatory molecules (Fig. 6d–f). Collectively, these data indicated that OA selectively activated the ERS pathway in activated HSCs.

Activation of ERS is required for OA to induce apoptosis in activated HSCs

Prolonged ERS triggers pro-apoptotic signals. However, ERS sensors do not directly lead to cell death. Instead, they stimulate the activation of downstream factors, such as CHOP, that promote the progression of cell death pathways [33]. Thus, we next investigated whether OA-mediated HSC apoptosis was dependent on ERS activation. Notably, immunofluorescence analysis showed that OA promoted the expression of CHOP and calnexin, but this effect was inhibited by treatment with salubrinal (Fig. S2A), a selective inhibitor that protects cells from ERS-induced apoptosis [34]. Similarly, OA at 40 μM markedly upregulated mRNA levels of both calnexin and CHOP in HSCs, but this was inhibited by salubrinal. However, OA did not significantly alter mRNA expression of calnexin and CHOP in LO_2 cells (Fig. S2B). Results of western blot analyses confirmed similar results at the protein level in HSCs (Fig. S2C). Our subsequent examinations showed that OA at 40 μM significantly promoted phosphorylation of PERK, and stimulated cleavage of ATF6 in HSCs. These results were consistent at the protein level, as demonstrated by western blot analyses (Fig. S2D–F). Collectively, our experiments showed that OA selectively activated the ERS pathway in HSCs.

The ERS signaling pathway results in caspase activation and, ultimately, the ordered and sequential dismantling of the cell [35]. Interestingly, caspase activation further promotes ERS. Using TUNEL staining to assess the nuclear morphology of apoptotic cells (Fig. 7a), we observed that OA induced HSC apoptosis, while salubrinal attenuated this proapoptotic effect. Further studies of apoptosis-regulating proteins showed that OA activated the caspase cascade and PARP, which was again attenuated by salubrinal (Fig. 7b–d). Next, we evaluated the expression of ECM components at mRNA and protein levels using western blot and qRT-PCR analyses, respectively. Interestingly, OA significantly reduced protein levels of intracellular α-SMA, type I collagen, and fibronectin compared with HSCs treated with DMSO, and salubrinal prevented this decrease in fibronectin and α-SMA levels (Fig. 7e). Coincidently, mRNA analysis

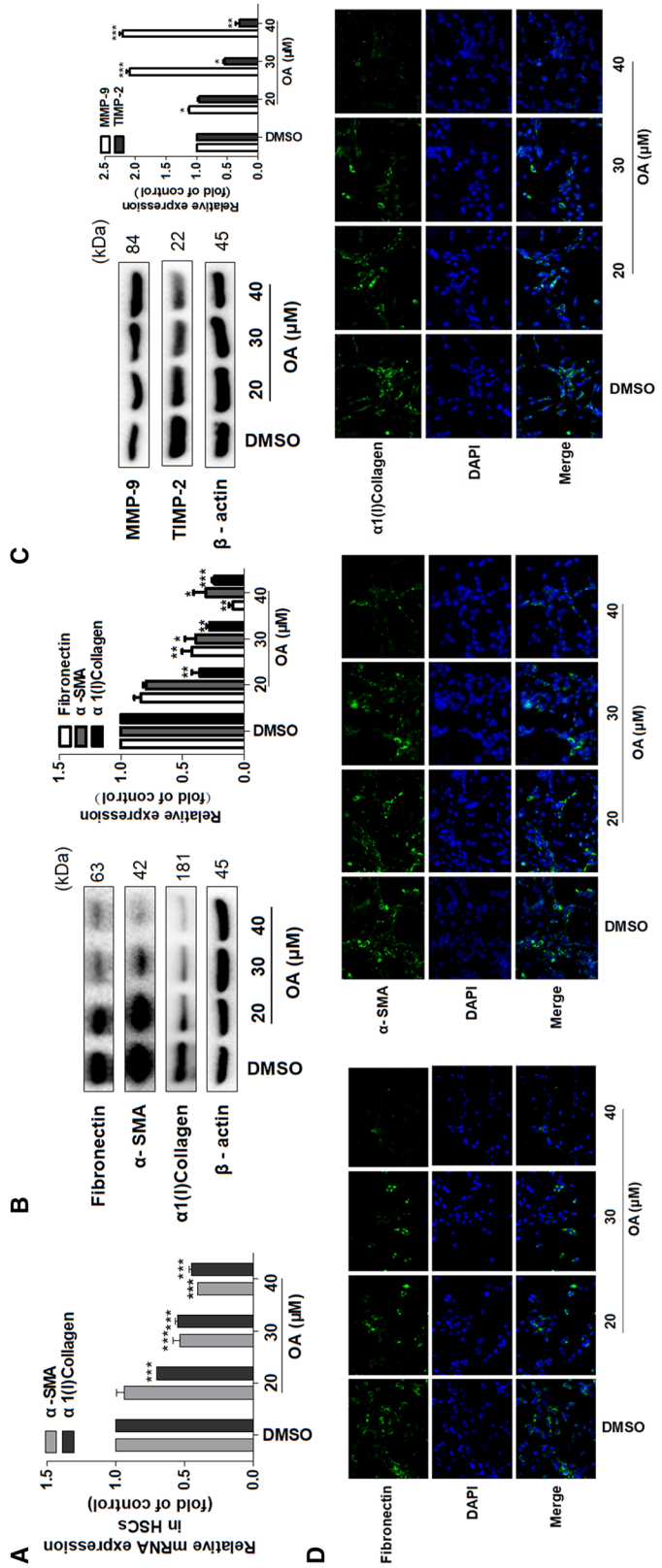

Fig. 5 OA inhibits HSC activation and reduces collagen deposition in vitro. HSCs were treated with DMSO (0.02%, w/v), or OA at indicated concentrations for 24 h. **a** The mRNA levels of type I collagen and α-SMA were determined using real-time PCR. **b** The protein levels of Fibronectin, type I collagen and α-SMA were measured by western blot. β-actin was used as a loading control. **c** OA regulated the expressions of TIMP-2 and MMP-9, as shown by western blot analysis. β-actin was used as a loading control. **d** Immunofluorescence analysis of Fibronectin, a-SMA and α1(I) procollagen (original magnification, ×40). Data are expressed as mean ± SD (n = 3); *P < 0.05, **P < 0.01 and ***P < 0.001 compared with DMSO

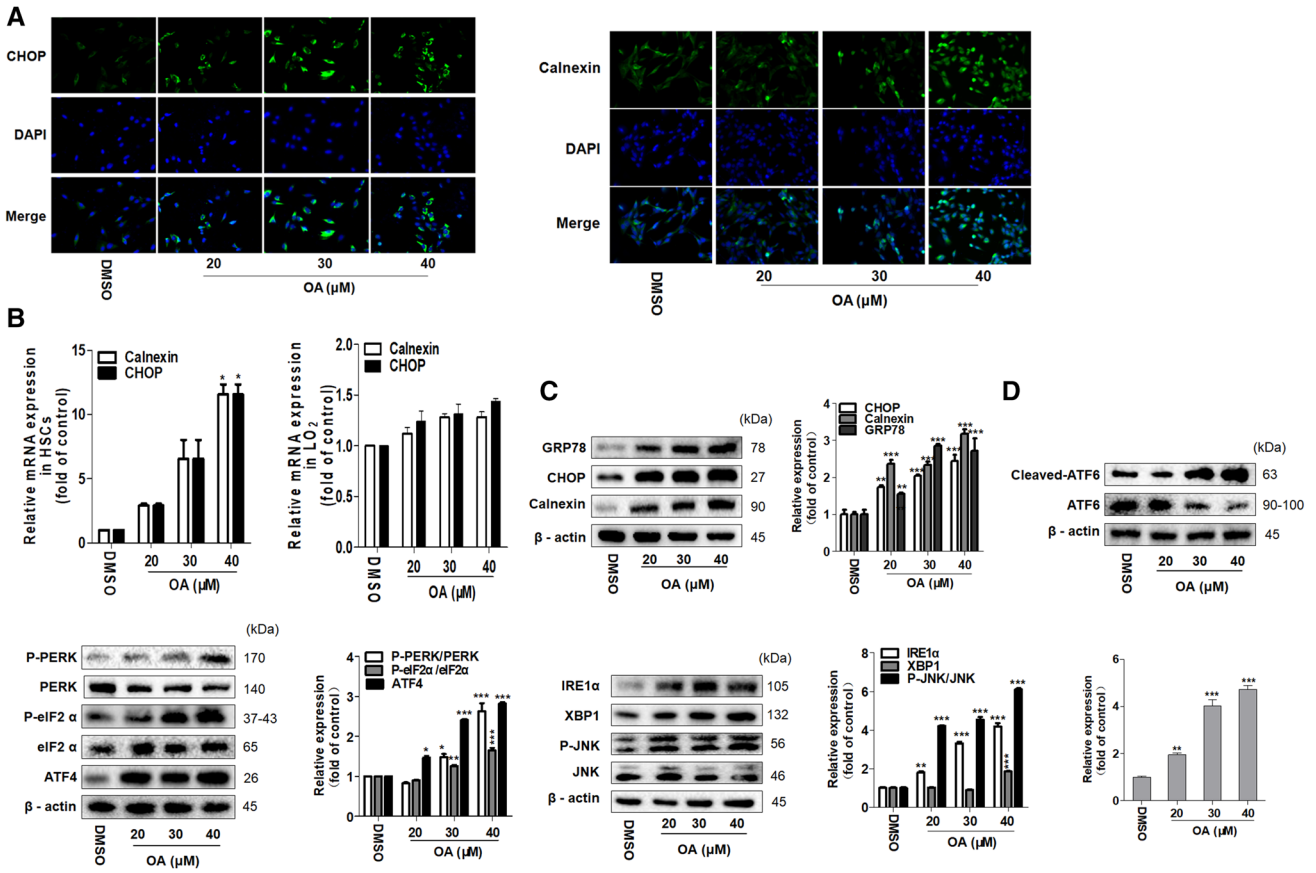

Fig. 6 OA activates ERS pathway in activated HSCs. **a** Immunofluorescence analysis of CHOP and Calnexin (original magnification, ×40). **b** Real-time PCR analyses of Calnexin and CHOP in HSC and human LO_2 hepatocytes. **c** Western blot analysis of ERS-associated proteins in HSC. **d**–**f** Western blot analyses of PERK, IRE1and ATF6 signaling pathway in HSC. Data are expressed as mean ± SD (n = 3); *P < 0.05, **P < 0.01 and ***P < 0.001 compared with DMSO

indicated that OA treatment resulted in decreased expression of both α-SMA and type I collagen, which was prevented by salubrinal (Fig. 7f). Taken together, our data indicated that OA triggered apoptosis through activation of the ERS pathway.

Activation of the ERS signaling pathway alleviated liver fibrotic injury and inflammatory reaction in mice

ERS is an early and essential biological event in tissue injury. Moderate ERS acts as a self-defense system and protects cells from injury, whereas over-activated ERS can lead to cell death by activating CHOP, JNK, and other signaling pathways [36]. Thus, we finally attempted to confirm these actions of OA in vivo using mice with CCl_4-induced hepatic fibrosis. Chronic liver disease is accompanied by inflammatory responses throughout the pathological process. Notably, OA improved CCl_4-induced liver inflammation. The inhibitory effect of OA on activation of proinflammatory signaling pathways and secretion of proinflammatory cytokines was diminished by salubrinal (Fig. 8a). In these mice, OA significantly decreased serum levels of ALT, ALP, AST, and LDH, and improved liver injury (Fig. 8b). Furthermore, H&E, Masson, and Sirius red staining showed that OA reduced CCl_4-induced excessive collagen deposition, which was partly abolished by salubrinal (Fig. 8c). Examination of key fibrogenic indicators indicated that serum levels of HA, LN, PCIII, and C-IV were decreased significantly by OA in fibrotic mice (Fig. 8d). Moreover, caspase-1 expression indicated OA reduced levels of inflammation (Fig. S3A). These alterations were further demonstrated in HSCs of intact mouse liver by immunofluorescence and western blot analyses (Figs. 8f, S3B), which were consistent with in vitro observations. Furthermore, upon detecting levels of inflammation, our results showed a clear increase in the level of proinflammatory cytokines in serum from Group 2, which was significantly decreased by OA treatment (Fig. S4). Collectively, these results provided further in vivo evidence that activation of ERS signaling inhibited the accumulation of collagen and alleviated inflammatory reactions in our mouse model of hepatic fibrosis.

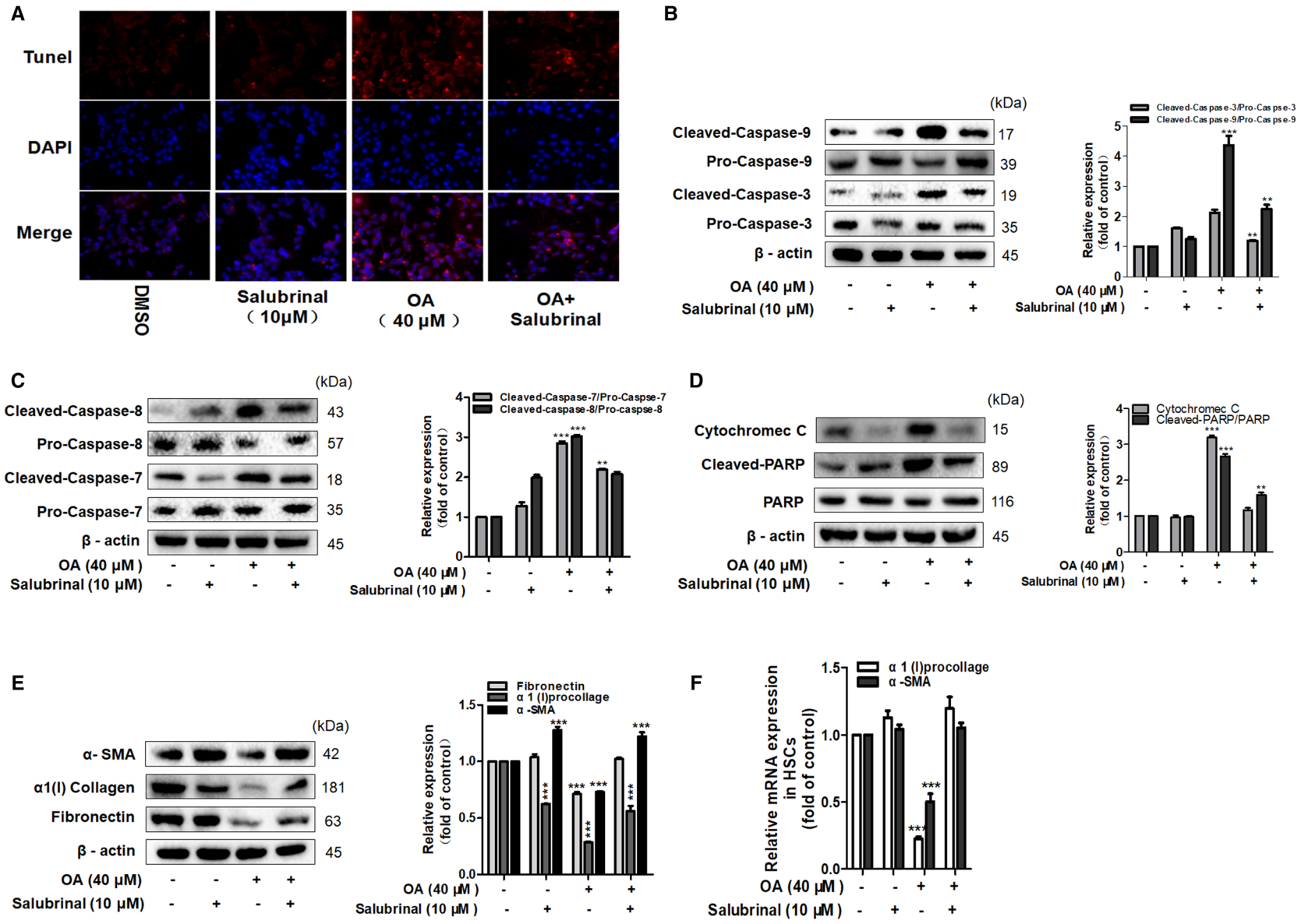

Fig. 7 The ERS signaling pathway leads to the HSC apoptosis and reduces collagen deposition induced by OA. HSCs were treated with DMSO (0.02%, w/v), OA or Salubrinal at indicated concentrations for 24 h. **a** TUNEL staining for evaluating HSC apoptosis. Red fluorescence indicated apoptotic cells (original magnification, ×40). **b–d** Western blot analyses of caspase cascades and PARP-1 in HSC. β-actin was used as an invariant control for equal loading. Representative blots were from three independent experiments. **e**, **f** Western blot and real-time PCR analyses of α1(I) procollagen and Fibronectin in HSC. Data are expressed as mean ± SD (n = 3); *P < 0.05, **P < 0.01 and ***P < 0.001 compared with DMSO

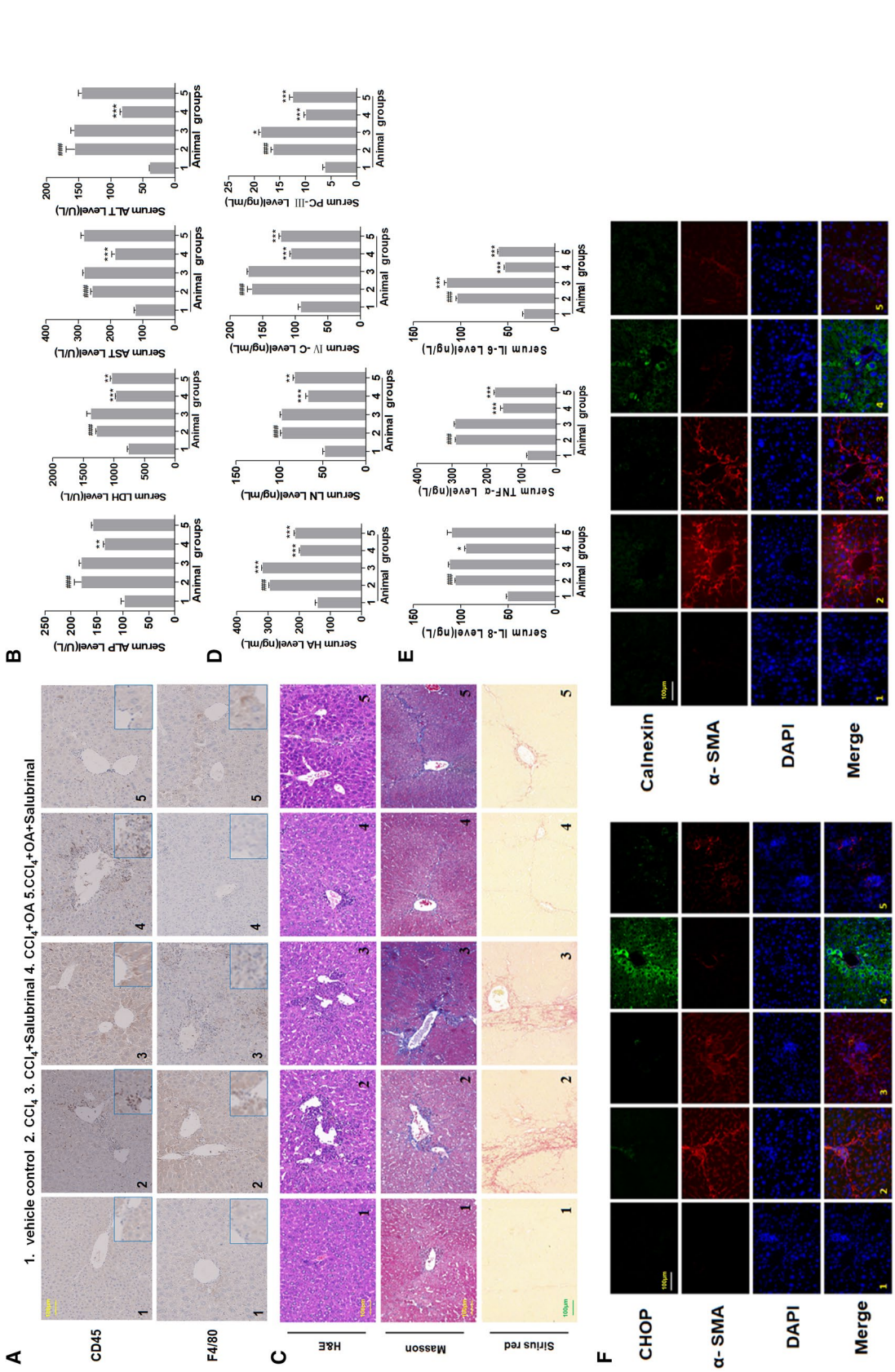

Fig. 8 Activation of the ERS signaling pathway alleviates liver fibrotic injury in mice. Mice were injected i.p. with CCl_4 for 8 weeks to induce hepatic fibrosis. During the weeks 5–8, mice in treatment groups were given OA (40 mg/kg) or Salubrinal (1 mg/kg). **a** Immunochemical staining for CD45 and F4/80 of liver sections (original magnification, ×20). **b** Determination of serum ALT, AST, ALP and LDH levels. **c** Liver sections were stained with hematoxylin and eosin, Masson reagents, Sirius red. Representative photographs are shown (original magnification, ×20). **d** Levels of HA, LN, PC-III, and C-IV in serum. **e** ELISA measurement of IL-6, IL-8 and TNF-α levels in liver and serum. **f** Liver sections were stained with Immunofluorescence using antibodies against CHOP and Calnexin. Antibody against α-SMA was used to specifically stain HSC, and DAPI to stain the nucleus (original magnification, ×40). Scale bar = 100 μm. For the statistics of each panel in this figure, data are expressed as mean ± SD (n = 8); $^{\#\#\#}P < 0.001$ compared with group one, $^{*}P < 0.05$, $^{**}P < 0.01$ and $^{***}P < 0.001$ compared with group two.

Discussion

Hepatic fibrosis might be prevented or even reversed by inducing apoptosis of activated HSCs. OA has been recognized as an important compound with a wide spectrum of pharmacological functions, including anti-cancer properties [9]. In this study, we established that OA induces apoptosis through ERS in activated HSCs, which may offer a new strategy for the treatment of hepatic fibrosis.

The production of ECM by activated HSCs, particularly type I collagen, plays an important role in hepatic fibrosis and cirrhosis [37]. Intact type I collagen promotes the persistence of activated HSCs, as ECM degradation is critical for induction of HSC apoptosis [38]. We discovered that OA decreased both mRNA and protein expression of α-SMA and type I collagen in activated HSCs. In the current study, OA significantly elevated the MMP-9/TIMP-2 ratio and altered the balance between collagen synthesis and degradation in activated HSCs in vitro. Thus, our results indicated that OA mediates the reduction of collagen deposition by directly decreasing type I collagen protein synthesis and indirectly increasing the MMP-9/TIMP-2 ratio, which potentially enhances ECM degradation.

We also found that OA upregulated the expression of ER-resident chaperones, such as CHOP, calnexin, and glucose-regulated protein 78 (GRP78). The signaling pathways involved this process represent adaptive responses to avoid unfolded proteins accumulation [39]. However, persistent activation of ERS leads to the failure of ER functions and cell death, typically through apoptosis [40]. As such, the role of ERS was further confirmed by evidence indicating that OA-induced HSC apoptosis was mediated through activation of the ERS pathway, and inhibited by salubrinal. In activated HSCs, salubrinal effectively attenuated OA-induced apoptosis and diminished expression of apoptotic markers, including cleaved PARP and caspase-3/9. These results strongly indicate that ERS is a key target to trigger apoptosis of activated HSCs. Interestingly, the proapoptotic effect of OA exhibited greater specificity for activated HSCs than hepatocytes. This is important, as during the progression of hepatic fibrosis, apoptosis of hepatocytes, which comprise the majority of the liver, should be prevented, while apoptosis of activated HSCs should be promoted. Our results indicated that low doses of OA caused significantly higher levels of apoptosis in activated HSCs, while apoptosis, proliferation, and inhibition of LO_2 were reduced compared with HSCs treated with the same dosage of OA. Thus, OA is an effective drug to induce apoptosis of activated HSCs while having little influence on hepatocyte vitality during treatment of hepatic fibrosis.

Our results indicated that OA had both antiproliferative and apoptosis-promoting effects on cultured HSCs. Moreover, OA inhibited collagen synthesis and induced collagen degradation in activated HSC. Furthermore, OA induced HSC apoptosis through a mechanism involving ERS and the caspase-dependent mitochondrial pathways.

Taken together, our study provides novel insights identifying ERS as a new pharmacologic target for the treatment of hepatic fibrosis. We also found that OA limited HSC activation through an ERS-dependent pathway in vivo and in vitro, suggesting OA should be further investigated as a prospective therapeutic agent for the treatment of hepatic fibrosis.

Acknowledgements This work was supported by the National Natural Science Foundation of China (81270514, 31401210, 31571455), Science and Technology Plan Program of Fujian Province (2017Y0061), Scientific Research Foundation of Third Institute of Oceanography, the Ministry of Natural Resources (2018020),Youth Natural Science Foundation of Jiangsu Province (BK20140955), Priority Academic Program Development of Jiangsu Higher Education Institutions, 2013 Program for Excellent Scientific and Technological Innovation Team of Jiangsu Higher Education, Natural Science Research General Program of Jiangsu Higher Education Institutions (14KJB310011), Top-notch Academic Programs Project of Jiangsu Higher Education Institutions (TAPPPPZY2015A070), and Open Project Program of Jiangsu Key Laboratory for Pharmacology and Safety Evaluation of Chinese Materia Medica (JKLPSE201502).

Compliance with ethical standards

Conflict of interest The authors declare that they have no conflicts of interest.

References

1. Kisseleva T, Brenner DA (2006) Hepatic stellate cells and the reversal of fibrosis. J Gastroenterol Hepatol 21(Suppl 3):S84–S87. https://doi.org/10.1111/j.1440-1746.2006.04584.x
2. Lee UE, Friedman SL (2011) Mechanisms of hepatic fibrogenesis. Best Pract Res Clin Gastroenterol 25(2):195–206. https://doi.org/10.1016/j.bpg.2011.02.005
3. Pradere JP, Kluwe J, De Minicis S, Jiao JJ, Gwak GY, Dapito DH, Jang MK, Guenther ND, Mederacke I, Friedman R, Dragomir AC, Aloman C, Schwabe RF (2013) Hepatic macrophages but not dendritic cells contribute to liver fibrosis by promoting the survival of activated hepatic stellate cells in mice. Hepatology 58(4):1461–1473. https://doi.org/10.1002/hep.26429
4. Roderburg C, Luedde M, Vargas Cardenas D, Vucur M, Mollnow T, Zimmermann HW, Koch A, Hellerbrand C, Weiskirchen R, Frey N, Tacke F, Trautwein C, Luedde T (2013) miR-133a mediates TGF-beta-dependent derepression of collagen synthesis in hepatic stellate cells during liver fibrosis. J Hepatol 58(4):736–742. https://doi.org/10.1016/j.jhep.2012.11.022
5. Novo E, Marra F, Zamara E, Valfre di Bonzo L, Monitillo L, Cannito S, Petrai I, Mazzocca A, Bonacchi A, De Franco RS, Colombatto S, Autelli R, Pinzani M, Parola M (2006) Overexpression of Bcl-2 by activated human hepatic stellate cells: resistance to apoptosis as a mechanism of progressive hepatic fibrogenesis in humans. Gut 55(8):1174–1182. https://doi.org/10.1136/gut.2005.082701

6. Bian M, Chen X, Zhang C, Jin H, Wang F, Shao J, Chen A, Zhang F, Zheng S (2017) Magnesium isoglycyrrhizinate promotes the activated hepatic stellate cells apoptosis via endoplasmic reticulum stress and ameliorates fibrogenesis in vitro and in vivo. Biofactors 43(6):836–846. https://doi.org/10.1002/biof.1390
7. Hotamisligil GS (2010) Endoplasmic reticulum stress and the inflammatory basis of metabolic disease. Cell 140(6):900–917. https://doi.org/10.1016/j.cell.2010.02.034
8. Jalan R, De Chiara F, Balasubramaniyan V, Andreola F, Khetan V, Malago M, Pinzani M, Mookerjee RP, Rombouts K (2016) Ammonia produces pathological changes in human hepatic stellate cells and is a target for therapy of portal hypertension. J Hepatol 64(4):823–833. https://doi.org/10.1016/j.jhep.2015.11.019
9. Lu L, Guo Q, Zhao L (2016) Overview of Oroxylin A: a promising flavonoid compound. Phytother Res 30(11):1765–1774. https://doi.org/10.1002/ptr.5694
10. Li HB, Chen F (2005) Isolation and purification of baicalein, wogonin and oroxylin A from the medicinal plant *Scutellaria baicalensis* by high-speed counter-current chromatography. J Chromatogr A 1074(1–2):107–110
11. Xu W, Lu C, Zhang F, Shao J, Yao S, Zheng S (2017) Dihydroartemisinin counteracts fibrotic portal hypertension via farnesoid X receptor-dependent inhibition of hepatic stellate cell contraction. FEBS J 284(1):114–133. https://doi.org/10.1111/febs.13956
12. Zhang F, Zhang Z, Chen L, Kong D, Zhang X, Lu C, Lu Y, Zheng S (2014) Curcumin attenuates angiogenesis in liver fibrosis and inhibits angiogenic properties of hepatic stellate cells. J Cell Mol Med 18(7):1392–1406. https://doi.org/10.1111/jcmm.12286
13. Chen Q, Chen L, Wu X, Zhang F, Jin H, Lu C, Shao J, Kong D, Wu L, Zheng S (2016) Dihydroartemisinin prevents liver fibrosis in bile duct ligated rats by inducing hepatic stellate cell apoptosis through modulating the PI3K/Akt pathway. IUBMB Life 68(3):220–231. https://doi.org/10.1002/iub.1478
14. Abriss B, Hollweg G, Gressner AM, Weiskirchen R (2003) Adenoviral-mediated transfer of p53 or retinoblastoma protein blocks cell proliferation and induces apoptosis in culture-activated hepatic stellate cells. J Hepatol 38(2):169–178
15. Bai T, Lian LH, Wu YL, Wan Y, Nan JX (2013) Thymoquinone attenuates liver fibrosis via PI3K and TLR4 signaling pathways in activated hepatic stellate cells. Int Immunopharmacol 15(2):275–281. https://doi.org/10.1016/j.intimp.2012.12.020
16. Zhang Z, Guo M, Zhao S, Shao J, Zheng S (2016) ROS-JNK1/2-dependent activation of autophagy is required for the induction of anti-inflammatory effect of dihydroartemisinin in liver fibrosis. Free Radic Biol Med 101:272–283. https://doi.org/10.1016/j.freeradbiomed.2016.10.498
17. Berger C, Kannan R, Myneni S, Renner S, Shashidhara LS, Technau GM (2010) Cell cycle independent role of Cyclin E during neural cell fate specification in Drosophila is mediated by its regulation of Prospero function. Dev Biol 337(2):415–424. https://doi.org/10.1016/j.ydbio.2009.11.012
18. Mazumder S, Plesca D, Almasan A (2007) A jekyll and hyde role of cyclin E in the genotoxic stress response: switching from cell cycle control to apoptosis regulation. Cell Cycle 6(12):1437–1442
19. Gao C, Pang M, Zhou Z, Long S, Dong D, Yang J, Cao M, Zhang C, Han S, Li L (2015) Epidermal growth factor receptor-coamplified and overexpressed protein (VOPP1) is a putative oncogene in gastric cancer. Clin Exp Med 15(4):469–475. https://doi.org/10.1007/s10238-014-0320-7
20. Hengartner MO (2000) The biochemistry of apoptosis. Nature 407(6805):770–776. https://doi.org/10.1038/35037710
21. Zhou F, Yang Y, Xing D (2011) Bcl-2 and Bcl-xL play important roles in the crosstalk between autophagy and apoptosis. FEBS J 278(3):403–413. https://doi.org/10.1111/j.1742-4658.2010.07965.x
22. Zhang T, Zhao G, Zhu X, Jiang K, Wu H, Deng G, Qiu C (2019) Sodium selenite induces apoptosis via ROS-mediated NF-kappaB signaling and activation of the Bax-caspase-9-caspase-3 axis in 4T1 cells. J Cell Physiol 234(3):2511–2522. https://doi.org/10.1002/jcp.26783
23. Bruni E, Reichle A, Scimeca M, Bonanno E, Ghibelli L (2018) Lowering etoposide doses shifts cell demise from caspase-dependent to differentiation and caspase-3-independent apoptosis via DNA damage response, inducing AML culture extinction. Front Pharmacol 9:1307. https://doi.org/10.3389/fphar.2018.01307
24. Engert F, Schneider C, Weibeta LM, Probst M, Fulda S (2015) PARP inhibitors sensitize ewing sarcoma cells to temozolomide-induced apoptosis via the mitochondrial pathway. Mol Cancer Ther 14(12):2818–2830. https://doi.org/10.1158/1535-7163.MCT-15-0587
25. Monson T, Wright T, Galan HL, Reynolds PR, Arroyo JA (2017) Caspase dependent and independent mechanisms of apoptosis across gestation in a sheep model of placental insufficiency and intrauterine growth restriction. Apoptosis 22(5):710–718. https://doi.org/10.1007/s10495-017-1343-9
26. Yu Y, Xie Z, Wang J, Chen C, Du S, Chen P, Li B, Jin T, Zhao H (2016) Single-nucleotide polymorphisms of MMP2 in MMP/TIMP pathways associated with the risk of alcohol-induced osteonecrosis of the femoral head in Chinese males: A case-control study. Medicine 95(49):e5407. https://doi.org/10.1097/MD.0000000000005407
27. Peres RC, Line SR (2005) Analysis of MMP-9 and TIMP-2 gene promoter polymorphisms in individuals with hypodontia. Braz Dent J 16(3):231–236
28. Liu Q, Zhang X, Hu X, Dai L, Fu X, Zhang J, Ao Y (2016) Circular RNA related to the chondrocyte ECM regulates MMP13 expression by functioning as a MiR-136 'Sponge' in human cartilage degradation. Sci Rep 6:22572. https://doi.org/10.1038/srep22572
29. Tao YK, Yu PL, Bai YP, Yan ST, Zhao SP, Zhang GQ (2016) Role of PERK/eIF2alpha/CHOP endoplasmic reticulum stress pathway in oxidized low-density lipoprotein mediated induction of endothelial apoptosis. Biomed Environ Sci 29(12):868–876. https://doi.org/10.3967/bes2016.116
30. Ridler C (2017) Alzheimer disease: inhibition of IRE1 signalling reduces AD pathology. Nat Rev Neurol 13(5):258. https://doi.org/10.1038/nrneurol.2017.51
31. Lai WL, Wong NS (2008) The PERK/eIF2 alpha signaling pathway of unfolded protein response is essential for N-(4-hydroxyphenyl)retinamide (4HPR)-induced cytotoxicity in cancer cells. Exp Cell Res 314(8):1667–1682. https://doi.org/10.1016/j.yexcr.2008.02.002
32. Masouminia M, Samadzadeh S, Ebaee A, French BA, Tillman B, French SW (2016) Alcoholic steatohepatitis (ASH) causes more UPR-ER stress than non-alcoholic steatohepatitis (NASH). Exp Mol Pathol 101(2):201–206. https://doi.org/10.1016/j.yexmp.2016.08.002
33. Rani S, Sreenivasaiah PK, Cho C, Kim DH (2017) Salubrinal alleviates pressure overload-induced cardiac hypertrophy by inhibiting endoplasmic reticulum stress pathway. Mol Cells 40(1):66–72. https://doi.org/10.14348/molcells.2017.2259
34. Gong T, Wang Q, Lin Z, Chen ML, Sun GZ (2012) Endoplasmic reticulum (ER) stress inhibitor salubrinal protects against ceramide-induced SH-SY5Y cell death. Biochem Biophys Res Commun 427(3):461–465. https://doi.org/10.1016/j.bbrc.2012.08.068
35. McKimpson WM, Kitsis RN (2017) A new role for the ER unfolded protein response mediator ATF6: induction of a generalized antioxidant program. Circ Res 120(5):759–761. https://doi.org/10.1161/CIRCRESAHA.117.310577
36. Yin L, Dai Y, Cui Z, Jiang X, Liu W, Han F, Lin A, Cao J, Liu J (2017) The regulation of cellular apoptosis by the ROS-triggered

PERK/EIF2alpha/chop pathway plays a vital role in bisphenol A-induced male reproductive toxicity. Toxicol Appl Pharmacol 314:98–108. https://doi.org/10.1016/j.taap.2016.11.013

37. Furuhashi H, Tomita K, Teratani T, Shimizu M, Nishikawa M, Higashiyama M, Takajo T, Shirakabe K, Maruta K, Okada Y, Kurihara C, Watanabe C, Komoto S, Aosasa S, Nagao S, Yamamoto J, Miura S, Hokari R (2018) Vitamin A-coupled liposome system targeting free cholesterol accumulation in hepatic stellate cells offers a beneficial therapeutic strategy for liver fibrosis. Hepatol Res 48(5):397–407. https://doi.org/10.1111/hepr.13040
38. Higashi T, Friedman SL, Hoshida Y (2017) Hepatic stellate cells as key target in liver fibrosis. Adv Drug Deliv Rev 121:27–42. https://doi.org/10.1016/j.addr.2017.05.007
39. Li Y, Zheng GY, Liu Y (2016) Salubrinal protects human lens epithelial cells against endoplasmic reticulum stress-associated apoptosis. Zhonghua Yan Ke Za Zhi 52(6):437–443. https://doi.org/10.3760/cma.j.issn.0412-4081.2016.06.008
40. Zhang Z, Wei C, Zhou Y, Yan T, Wang Z, Li W, Zhao L (2017) Homocysteine induces apoptosis of human umbilical vein endothelial cells via mitochondrial dysfunction and endoplasmic reticulum stress. Oxid Med Cell Longev.https://doi.org/10.1155/2017/5736506